Optik 124 (2013) 4734–4738

Contents lists available at ScienceDirect

Optik

journal homepage: www.elsevier.de/ijleo

# Mapping of powdery mildew using multi-spectral HJ-CCD image in Beijing suburban area

Lin Yuan [a,b], Jingcheng Zhang [a,b,*], Jinling Zhao [a], Linsheng Huang [a,c], Xiaodong Yang [a], Jihua Wang [a,b]

[a] Beijing Research Center for Information Technology in Agriculture, Beijing 100097, China
[b] Institute of Agriculture Remote Sensing and Information System Application, Zhejiang University, Hangzhou 310029, China
[c] Key Laboratory of Intelligent Computing & Signal Processing, Ministry of Education, Anhui University, Hefei 230039, China

ARTICLE INFO

*Article history:*
Received 2 September 2012
Accepted 24 January 2013

*Keywords:*
Winter wheat
Powdery mildew
HJ-CCD
Spectral information divergence (SID)
Spectral angle mapper (SAM)

ABSTRACT

Powdery mildew is one of the most serious diseases, which has a significant impact on the production of winter wheat. As an effective alternative to traditional sampling methods, remote sensing can be a useful tool in disease detection. This study examines the potential of a moderate resolution multispectral satellite image in disease monitoring at regional scale. At the suburban area around Beijing, a large size ground survey sample ($n=90$) and the corresponding HJ-CCD image were acquired at the grain filling stage of winter wheat. A number of spectral features were found to be sensitive to powdery mildew through an independent $t$-test. Based on these spectral features, classification models were established using both spectral information divergence (SID) and spectral angle mapper (SAM), respectively. The results showed that the overall accuracies of disease identification and severity estimation were moderate. The estimation of normal and seriously infected samples yielded higher accuracies than slightly infected samples. The single phase HJ-CCD can only be used for locating the infected areas of powdery mildew, whereas is unable to discriminate the severity levels of disease. The presence of several stressors and disturbances other than disease is a possible reason of the unsatisfactory performance of disease monitoring models. Therefore, the integration of multi-phase onboard data and some relevant ancillary data is necessary to improve the accuracy and reliability of disease monitoring at regional scale.


## 1. Introduction

Crop diseases have a significant impact on the both yield and quality of crops around the world [1,2]. As an important disease of winter wheat, the powdery mildew (*Blumeria graminis*) is one of the most destructive diseases, which has a significant impact on the production of winter wheat. The disease distribution information is important for guiding the fungicide spray in early phase, and can also provide important information for yield loss assessment in later phase. However, for obtaining the spatial distribution of powdery mildew, the traditional disease scouting is not only time-consuming and labor-intensive, but also expensive and subjective, which thus cannot satisfy the demand of disease monitoring at a regional scale. As an emerging technology, remote sensing provides an alternative way to conduct disease monitoring in real-time [3].

A number of studies were carried out at leaf and canopy levels to identify some spectral features that were sensitive to diseases [4–6]. Based on these spectral features, several attempts were made in disease mapping with multispectral or hyperspectral images. Qin and Zhang used multispectral airborne imagery to monitor the infestation of rice sheath blight [7]. Huang et al. achieved high accuracies by applying an airborne hyperspectral data in detecting yellow rust at field level, with the $R^2$ of models over 0.9 [8]. Yang et al. distinguished cotton root rot using hyperspectral and multispectral airborne images [9]. Both data are able to quantify the disease infestation with satisfactory accuracies.

However, it should be noted that most of studies in disease detecting at field level utilized airborne imagery as data source. This sort of data is always expensive to acquire yet only covers small area, which cannot be widely used at regional scale. Comparatively, some moderate resolution multispectral satellite images, e. p. Landsat TM, represent a good compromise between spatial resolution and spatial extent for mapping the distribution of some crop diseases. Moreover, these onboard data are much cheaper and easier to be preprocessed than airborne imagery. However, limited to our knowledge, the studies that used satellite images for disease monitoring at regional scale are very rare.

In this study, the powdery mildew in winter wheat was selected as an example because it leads to a contiguous stretched landscape characteristics in the field, which is suitable for the multispectral data at moderate spatial resolution. The domestic satellite data, HuanJing CCD images (using HJ-CCD for short in the following) were adopted as the remote sensing data, which is a multispectral image

* Corresponding author at: Beijing Research Center for Information Technology in Agriculture, Beijing 100097, China.
*E-mail address:* zhangjc@nercita.org.cn (J. Zhang).

0030-4026/$ – see front matter © 2013 Elsevier GmbH. All rights reserved.
http://dx.doi.org/10.1016/j.ijleo.2013.01.103

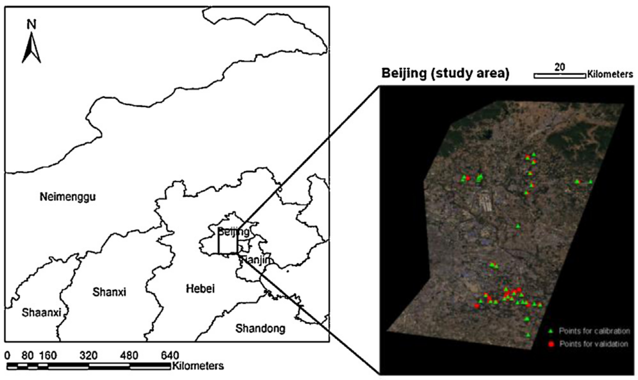


**Fig. 1.** Map of study area and the distribution of surveyed plots. Note: (A) generated by SID; (B) generated by SAM.

with similar spatial resolution (30 m) with Landsat-5 TM. The high revisit frequency (4 days) and wide swath width (360 km) makes it a reasonable onboard data for agricultural monitoring. The objectives of this study are: (1) to examine the sensitivity of a series of commonly used spectral features to powdery mildew at regional level; (2) to examine the performance of HJ-CCD in the monitoring of powdery mildew.

## 2. Methods

### 2.1. Study site

The study site was selected at the suburbs around Beijing, which covered Tongzhou and Shunyi counties (Fig. 1). During October to June, winter wheat is the major crop in this site. Given the climate characteristics of high humidity and rainfall, the powdery mildew occurs almost every year in this area.

### 2.2. Image data and field investigation

In field, the development of powdery mildew shows a significant temporal pattern during the growth stage of winter wheat. The symptom of plants was unobvious before booting stage, and was then developing rapidly and was peaking at filling stage. At a later time, with the plants turning yellow due to maturity, the disease characteristics gradually vanished as the milk stage starts. Therefore, the filling stage was chosen to conduct the ground survey, when the symptom of disease is most significant in the field.

One scene of cloud-free HJ-CCD on May 25, 2010 (ID: 308,679) was acquired and preprocessed for disease monitoring. The preprocessing procedures included calibration, atmospheric correction and geometric correction. The calibration coefficients (including bias and gain) were provided by the China Center for Resource Satellite Data and Applications. The calibrated data were atmospherically corrected with the algorithm provided by Liang et al., which estimated the spatial distribution of atmospheric aerosols and retrieved surface reflectance under general atmospheric and surface conditions [10]. Then the atmospherically corrected data was geometric corrected against a historical Landsat ETM+ image with precise coordinate information by using 80 ground control points. The root mean square error for the geometric corrected scene was less than 15 m. After that, the objects other than winter wheat were masked out using a decision tree classification method. The subsequent analysis is only implemented in the pure wheat planting regions.

The ground survey of powdery mildew was carried out on May 26–28 in 2010, with no more than 3 days to the date when the image was acquired. Within the study area, a total of 90 plots were randomly selected and surveyed (Fig. 1). In them, 54 samples were used for calibration, whereas the other 36 samples were used for validation. We classified each plot into normal (non-infected), slight (0–30% of the plot was infected), or heavy (over 30% of the plot was infected) classes, based on Li et al.'s criterion [11].

### 2.3. Spectral features for disease monitoring

In addition to the four original bands of HJ-CCD, we also included nine multi-spectral vegetation indices (VIs) for detecting powdery mildew, which were simple ratio (SR), normalized difference vegetation index (NDVI), green normalized difference vegetation index (GNDVI), triangular vegetation index (TVI), soil adjusted vegetation index (SAVI), optimized soil adjusted vegetation index (OSAVI), modified simple ratio (MSR), non-linear vegetation index (NLI) and re-normalized difference vegetation index (RDVI) (Table 1). Some of these VIs were proved to be responsible for the plant stress status, such as NDVI and TVI [12,13]. Others, such as SR, NDVI and GNDVI were used for detecting plant diseases [12,14].

To examine the sensitivity of the above spectral features to powdery mildew, an independent *t*-test was adopted by comparing a feature at normal and diseased points, based on the ground survey data.

### 2.4. Algorithms for disease monitoring

Two methods were tested for their performances in disease detection, including the spectral information divergence (SID) and the spectral angle mapper (SAM). Both algorithms were proven to be efficient in information extraction in several cases [25–27]. They are able to estimate disease severity for an untested pixel, based on the sample for calibration.

SID is actually a spectral similarity measure to capture the spectral correlation between two pixels. Assume $x$ and $y$ are vectors that indicating two pixels with $l$ bands. $p$ and $q$ are their probability vectors. Based on the information theory, the relative entropy can be delineated as:

$$D\ (x\|\,y) = \sum_{l}^{L} p_l D_l(x\|\,y) = \sum_{l}^{L} p_l(I_l(y) - I_l(x)) = \sum_{l}^{L} p_l \log\left(\frac{p_l}{q_l}\right) \quad (1)$$

where $D\,(x||y)$ is the cross-entropy. Based on which, the SID can be defined as:

$$\mathrm{SID}\ (x, y) = D(x\|\,y) + D(y\|\,x)\infty \quad (2)$$

SID provides a measure of spectral similarity by utilizing relative entropy to account for the spectral information of each pixel. A more detailed description of SID can be found in Chang's study [28].

The SAM is a physically-based spectral classification that uses an n-dimensional angle to match pixels to reference spectra. The spectral angle between two pixels can be calculated by the following formula:

$$\theta = \arccos \frac{\sum_{i=1}^{4} x_i x_{Ri}}{\sqrt{\sum_{i=1}^{4} x_i^2}\sqrt{\sum_{i=1}^{4} x_{Ri}^2}} \quad (3)$$

### 2.5. Methods of accuracy assessment

The performance of SID and SAM in disease detection was assessed and compared through a number of accuracy indicators, including overall accuracy (OAA), average accuracy (AA), producer's accuracy, user's accuracy and *kappa* coefficient.